Chaos, Solitons and Fractals 140 (2020) 110169

Contents lists available at ScienceDirect

Chaos, Solitons and Fractals

Nonlinear Science, and Nonequilibrium and Complex Phenomena

journal homepage: www.elsevier.com/locate/chaos

Wandering walk of chimera states in a continuous medium

A.J. Alvarez-Socorro[a,b,*], M.G. Clerc[a], M.A. Ferré[a]

[a] Departamento de Física and Millennium Institute for Research in Optics, Facultad de Ciencias Físicas y Matemáticas, Universidad de Chile, Santiago, Chile
[b] Laboratorio de Investigacin, Desarrollo e Innovación, Zenta Group, Andrés Bello 2687, Las Condes, Santiago, Chile

ARTICLE INFO

Article history:
Received 16 July 2020
Accepted 27 July 2020

Keywords:
Localized structures
Chimeras
Nonvariational effects
Wandering walks
Spatiotemporal chaos

ABSTRACT

The coexistence of coherent and incoherent domains in discrete coupled oscillators, *chimera state*, has been attracted the attention of the scientific community. Here we investigate the macroscopic dynamics of the continuous counterpart of this phenomenon. Based on a prototype model of pattern formation, we study a family of localized states. These localized solutions can be characterized by their sizes, and positions, and Yorke-Kaplan dimension. Chimera states in continuous media correspond to chaotic localized states. As a function of parameters and their size, the position of these chimera states can be bounded or unbounded. This allows us to classify these solutions as wandering or confined walk. The wandering walk is characterized by a chaotic motion with a truncated Gaussian distribution in its displacement as well as memory effects.

Localized structures are a characteristic feature of the self-organized non-equilibrium systems [1–3]. These structures, described as particle-like solutions, are characterized by continuous order parameters like the position, width, and amplitude [4]. Notwithstanding, localized structures corresponds to extended solutions. They have been observed in numerous fields, ranging from physics, chemistry to biology [4–6]. The localized structures are the dissipative counterpart of the solitons in conservative systems. In one-dimensional systems, they can be interpreted as spatial trajectories that connect one steady state with itself. Indeed, they are homoclinic orbits of the spatial co-moving system [7]. Localized structures are not necessarily motionless. As a result of symmetry breaking instabilities, they can exhibit motion or self-pulsation [8–14]. Recently, it has been shown that parity symmetry breaking induces spontaneous motion of localized structures [15]. A unified description of localized structures and their dynamic behavior can be achieved by the nonvariational Swift-Hohenberg equation [16–19]. This model accounts for a scalar field that does not follow minimization principles. The nonvariational Swift-Hohenberg equation has been derived in several contexts [19]. Moreover, this equation is used to puts light on the existence, stability properties, and dynamical evolution of complex spatiotemporal localized structures called *chaoticons* [20]. This intriguing phenomenon is observed in a liquid crystal light valve experiment with optical feedback. Furthermore, numerically chaoticons are obtained in nonlocal nonlinear Schrödinger equation [22], Ginzburg-Landau equation [21] and a reaction-diffusion model [23]. Indeed, these states show a coexistence between coherence (stationary) and incoherence (spatiotemporal chaotic) domains. Hence, chaoticons are the continuous counterpart of chimera states [24], namely, chaoticons correspond to chimera-like solutions. Originally, chimera states were observed in nonlocally coupled phase oscillators [25]. These intrigued states correspond to breaking symmetry solution without bistability. Extension of chimera states in bistable systems was proposed in several coupled systems [26–29], which was usually denominated chimera-like states. Depending on the initial condition, these states have different size and exhibit a family of solutions with the coexistence of coherent and incoherent domains.

Since then, chimera states have been investigated in more general frameworks [30–35]. Initially, even though the existence of chimera states was attributed to the nonlocal nature of the coupling [24]. Subsequently, chimera states have been observed in systems that are coupled globally [36–38], and locally [26–28,39,40,21]. In all these studies, domains remain motionless. However, under special conditions, chimera states are traveling solutions. This is observed under symmetric [41,42] and asymmetric schemes of coupling [29,43–45]. Even, chimera states show an erratic motion with stochastic nature in a finite number of coupled oscillators [42,46]. This fact is reflected by the loss of memory of the chimera position, which is counterintuitive for a deterministic system. Henceforth in this manuscript, we will use the term

* Corresponding author.
E-mail address: alejandro.alvarez@ing.uchile.cl (A.J. Alvarez-Socorro).

https://doi.org/10.1016/j.chaos.2020.110169
0960-0779/

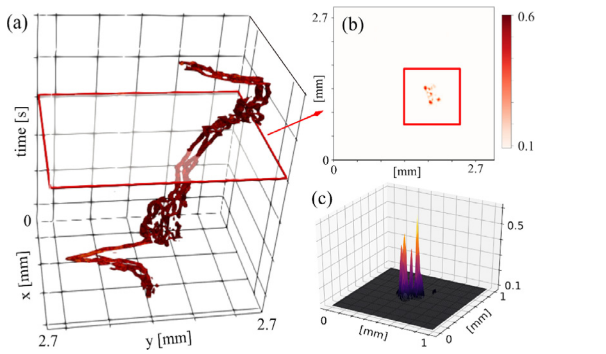

Fig. 1. (color online) Experimental observation of an erratic walk of a localized spot in a liquid crystal light valve with optical feedback. (a) Experimental spatiotemporal evolution of a localized spot. (b) Instantaneous snapshot of the localized state. (c) A plot of the light intensity at a given time (Courtesy of Nicolas Verschueren).

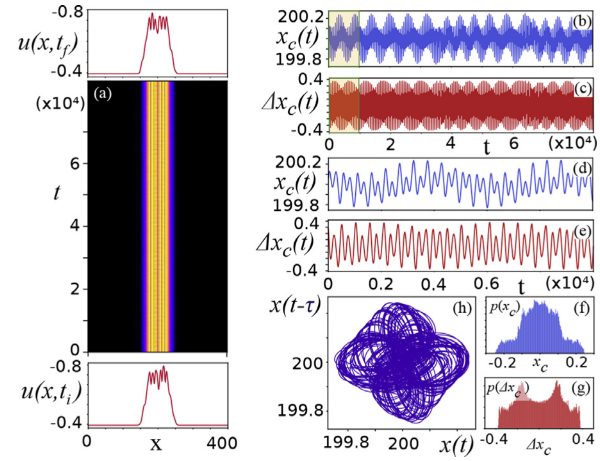

Fig. 2. (color online) Confined chimera states observed in the Swift-Hohenberg Eq. (1) by $\eta = -0.09$, $\mu = -0.04$, $\nu = 1$, $b = -2$, $c = 21$, $dx = 0.6$ and $dt = 0.01$. (a) Spatiotemporal evolution of a confined chimera state of 6 bumps. Temporal evolution of the centroid (b) and displacement (c) of the chimera state. Panels (d) and (e) show, respectively, an excerpt of the centroid and displacement for the first 10^4 time steps. (f) and (g) are the statistical distribution for centroid and displacements of chimera state, respectively. (h) Phase portrait reconstruction in 2D space of chimera state centroid.

chimera to refer a complex spatiotemporal localized state in continuous media.

Unexpectedly, in a liquid crystal light valve experiment with optical feedback, an erratic walk dynamics of chaoticons is observed (see Fig. 1). This complex walk accounts for an erratic motion of the position of the complex localized structure. This dynamic is of deterministic nature. Theoretically, the chaoticon was described by the non-variational Swift-Hohenberg equation [20]. However, the reported dynamics of chaoticons of this model are characterized by erratic localized fluctuations in a bounded region of the order of one wavelength of the spatiotemporal chaotic state [20], at variance to the experimental observations characterized by an unbounded erratic walk. The mechanism that produces these states and their dynamics is an open problem.

In this paper, we investigate the erratic walk of chimera states in continuous media. Based on a prototype model of localized structures—the non-variational Swift-Hohenberg equation—we numerically observe and analyze wandering walks of localized structures. To characterize this wandering motion, we use tools of the dynamical systems and statistics theory. Finally, in comparison to the random dynamics of chimera states in coupled oscillators [46], the motion of the wandering walk of chimera-like state shows memory effects. Namely, the self-correlation of the position of this localized state does not become zero.

An archetypal model that shows patterns, fronts, localized structures, and chimera-like states in continuous media is the non-variational Swift-Hohenberg equation [19,20,47,48]. It describes the dynamics near a Lifshitz critical point [2] that accounts for the confluence of a spatial instability and a nascent of bistability through the scalar order parameter $u(x, t)$,

$$\partial_t u = \eta + \mu u - u^3 - \nu \partial_{xx} u - \partial_{xxxx} u + c(\partial_x u)^2 + 2bu\partial_{xx} u, \qquad (1)$$

where x and t stand for the spatial and temporal coordinates, respectively. μ is the bifurcation parameter ($\mu \ll 1$), η accounts for the asymmetry between homogeneous states, c, ν, and b are, respectively, the nonlinear advection, the linear and the nonlinear diffusion coefficients. The term proportional to the four spatial derivative accounts for the hyperdiffusion. Higher-order terms in Eq. (1) are ruled out by scaling analysis, since $u \sim \mu^{1/2}$, $\eta \sim \mu^{3/2}$, $\nu \sim \mu^{1/2}$, $\partial_t \sim \mu$, $\partial_x \sim \mu^{1/4}$, and $c \sim b \sim O(1)$.

When $b = c = \eta = 0$, Eq. (1) corresponds to the well-known Swift-Hohenberg model [2,49]. The minimization of free energy characterizes the dynamics of Eq. (1). Hence, the Swift-Hohenberg equation shown only stationary solutions as equilibria. Indeed, this dynamics is of variational nature. However, in the case that $b \neq c$, model Eq. (1) losses its variational structure, allowing the existence of solutions that show permanent dynamics, such as propagative fronts [50], moving and oscillatory localized structures [15,48,51], and chimera-like states [20]. Fig. 2(a) displays a typical chimera state of model Eq. (1). This dynamic behavior is characterized by presenting localized spatiotemporal chaos, which is surrounded by homogeneous states on its flanks. It is noteworthy to note that despite its spatiotemporal complexity, the evolution of the chimera state position is localized in space, that is, the localized state is confined. To characterize the dynamics of the chimera state, let us introduce its position or centroid as

$$x_c(t) = \frac{\int_{-L}^{L} x\hat{u}(x,t)dx}{\int_{-L}^{L} \hat{u}(x,t)dx}, \qquad (2)$$

where $\hat{u}(x,t) \equiv u(x,t) + h$ and h is the distance of the homogeneous state to zero. Moreover, we consider displacements of chimera state Δx_c, taking the difference of its position between two successive time steps.

Fig. 2 shows the temporal evolution of the centroid and displacements of the chimera state. These dynamics reveal a rich and complex evolution. Note that the dynamics of the centroid is bounded by one wavelength. Hence, the chimera state remains around a given position. The statistical characterization of the centroid and displacements dynamics are shown in Fig. 2(f) and (g), respectively. In both cases, the distributions are bounded, reflecting the fact that the spatiotemporal chaotic localized structure is pinned. The richness and complexity of such kind chaotic localized structures have been studied previously in Verschueren et al. [20]. The reconstruction of the attractor for the centroid of chimera state—following the classical Fraser and Swinney method [53]—obtaining by unfolding in a 2D space is shown in Fig. 2(h). Unexpectedly, when changing parameters, the position of the chimera exhibits complex behaviors, which causes the chimera to move distances greater than the characteristic wavelength of the spatiotemporal chaotic state (cf. right panels in Fig. 3).

To the best of our knowledge, the complex and unbounded dynamical behavior of the position of chimera states has not been reported in continuous media. To investigate such localized structures dynamics, we have conducted a numerical analysis of model Eq. (1) in the nonvariational regime. For the sake of simplicity, periodic boundary conditions have been considered, however, similar dynamic behaviors are observed with other boundary conditions. Fourth-order Runge-Kutta in time and finite differences in space

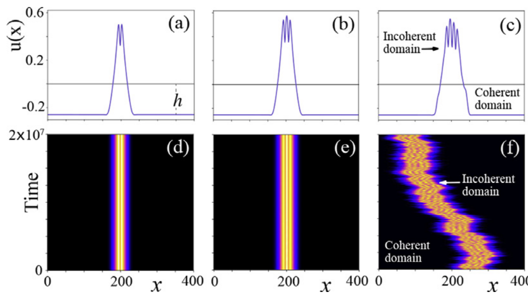

Fig. 3. (color online) Single localized structures of the non-variational Swift-Hohenberg Eq. (1) by $\eta = -0.04$, $\mu = -0.09$, $\nu = 1$, $b = -2$, $c = 24$, $dx = 0.4$ and $dt = 0.001$. (a) Profile and (d) spatiotemporal evolution of the motionless localized structure with two bumps. h is the distance of the homogeneous state to zero. (b) Profile and (e) spatiotemporal evolution of the motionless localized structure with three bumps. The position or centroid of the localized structure is maintained at a fixed location. Besides, the heights of the bumps oscillate with a fixed amplitude and frequency. (c) Profile and (f) spatiotemporal evolution of the wandering complex localized solution. This state has four bumps. Each of them exhibits complex aperiodic oscillations, while the localized structure changes its position erratically. Here the coherent domain has a constant dynamics, whereas the incoherent domain has complex dynamical behavior.

are the numerical methods used to integrate model Eq. (1). In all simulations, the space is discretized in 400 points with $dx = 0.4$, and the time step size is $dt = 0.001$. Fig. 3 shows typical localized solutions exhibited by the model Eq. (1). The system shows only these three types of single localized states in a given region of parameters. These localized solutions as a function of their width are characterized by being stationary, oscillatory, or chaotic, respectively. Other localized states are a composition of these simple solutions. The top panels in Fig. 3 show profiles of each localized structure at a given time, and the bottom panels display the respective spatiotemporal evolution of localized states. Solutions that have two and three bumps correspond to stationary states, depicted in Fig. 3(d) and (e). However, a complex spatiotemporal evolution is shown by the localized structure that exhibits four bumps, see Fig. 3(f). In the former case, the system shows coexistence between coherent and incoherent domains. Indeed, this state corresponds to a chimera state, but instead of the chimera state shown in Fig. 2, it exhibits a wandering walk in its position, which is characterized by move several times the characteristic wavelength of the chaotic domain. Hence, the incoherence domain presents wandering movements which resemble a random walk [52].

Fig. 4 illustrates the temporal evolution of the four-bumps chimera solution and its respective centroid $x_c(t)$. To figure out the sensitivity of the initial conditions on the motion of this chimera state the position $x_c(t)$ is calculated for slightly different initial conditions [see Fig. 4(c)]. From this figure, one can infer that the position of the chimera solution presents complex dynamics as a function of the initial conditions. Likewise, to reveal the nature of the movements, we compute its displacements, taking the difference of its position between two successive time steps. Hence, the displacements are defined by $\Delta x(t) \equiv x_c(t) - x_c(t-\tau)$. Fig. 5 shows the temporal evolution of the displacement $\Delta x(t)$ and its respective histogram which has a bell shape. Building the associated distribution of displacements, we found that a Gaussian distribution well describes it. Consider a fitting distribution function of the form

$$f(\Delta x) = \frac{1}{\beta\sqrt{2\pi}} e^{-\frac{(\Delta x-\mu)^2}{2\beta}}, \tag{3}$$

where μ corresponds to the mean value of the displacements ($\mu \equiv \langle \Delta x \rangle$, where the symbol $\langle \cdot \rangle$ accounts for the average on the values of the displacements). β accounts for the standard deviation. The probability density distribution, and the Gaussian func-

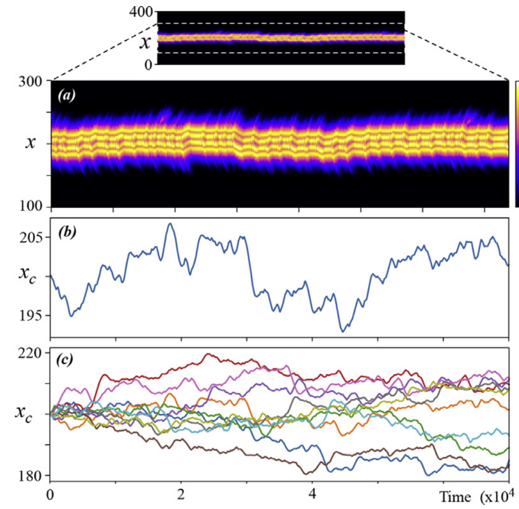

Fig. 4. (color online) Wandering walk of chimera states of the non-variational Swift-Hohenberg Eq. (1) by $\eta = -0.04$, $\mu = -0.09$, $\nu = 1$, $b = -2$, $c = 24$, $dx = 0.4$ and $dt = 0.001$. (a) Excerpts of Spatiotemporal diagram of a wandering chimera state. (b) Temporal evolution of the centroid $x_c(t)$ of the chimera state, calculated using formula (2), of the respective spatiotemporal evolution presented in panel (a). (c) Several trajectories of the centroid of chimera state calculated for different slightly initial conditions.

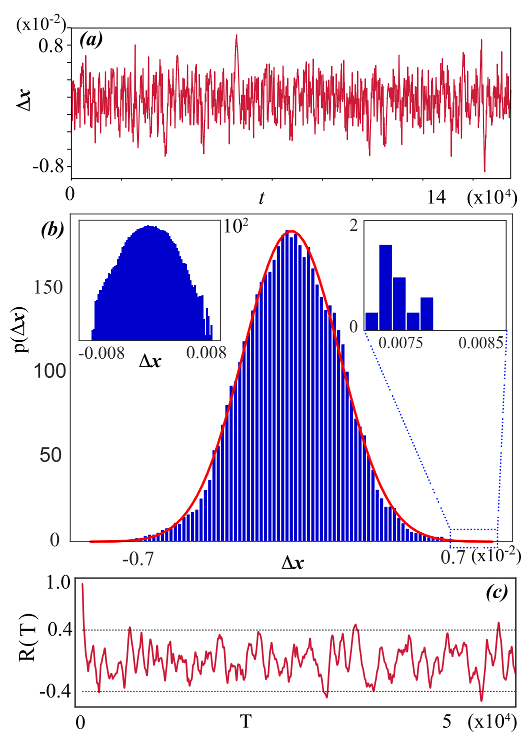

Fig. 5. (color online) Statistical characterization of displacements of the position of the chimera solution $\Delta x(t)$ for Eq. (1) with $\eta = -0.04$, $\mu = -0.09$, $\nu = 1$, $b = -2$, $c = 24$, $dx = 0.4$ and $dt = 0.001$. (a) Longtime evolution of the displacements $\Delta x(t)$. (b) The probability distribution of displacements, which shows a Gaussian-like distribution. The continuous curve (red) accounts for a Gaussian adjustment function, formula (3), with $\mu \approx 0$ and $\beta \approx 2.158 \times 10^{-3}$. The left inset shows the probability distribution of displacements in the log-log scale. This illustrates that the distribution corresponds to a truncated Gaussian. The right inset shows amplification of the tails of the distribution. (c) Self-correlation function $R(T)$ based on Pearson's coefficient. The fact that this function does not decay to zero highlight the memory effects of the wandering motion of chimera states. (For interpretation of the references to color in this figure legend, the reader is referred to the web version of this article.)

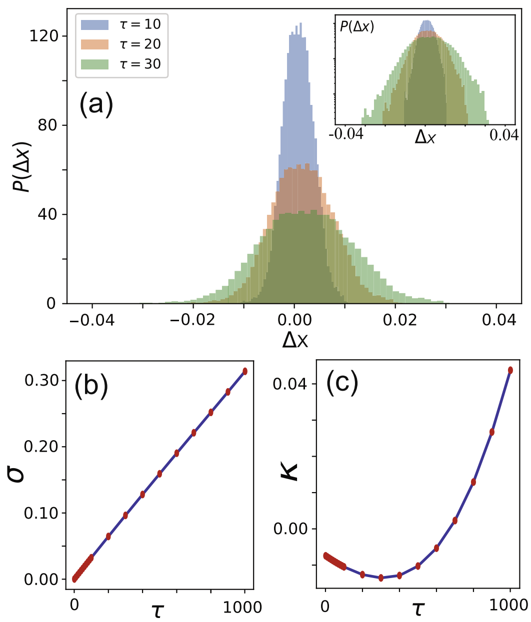

Fig. 6. (color online) Temporal characterization of statistical measures of wandering chimera states for model Eq. (1) by $\eta = -0.04$, $\mu = -0.09$, $\nu = 1$, $b = -2$, $c = 24$, $dx = 0.4$ and $dt = 0.001$. (a) Displacement distributions for different waiting times $\tau = 10$, 20, and 30, respectively. Temporal evolution of the standard deviation (b), and the excess kurtosis (c).

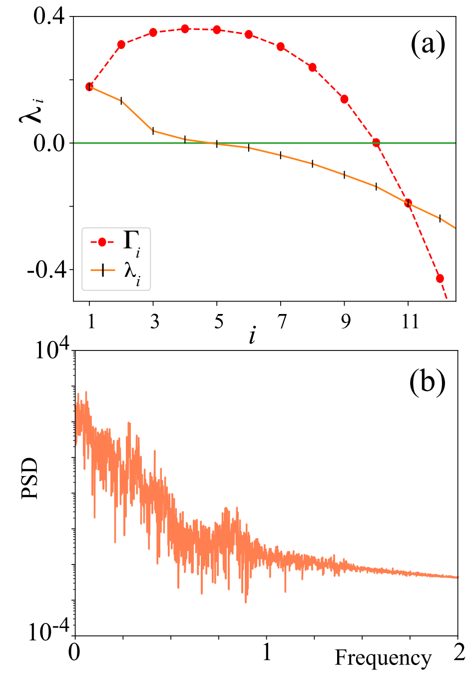

Fig. 7. (color online) Dynamic characterization of the wandering chimera state of the non-variational Swift-Hohenberg Eq. (1) by $\eta = -0.04$, $\mu = -0.09$, $\nu = 1$, $b = -2$, $c = 24$, $dx = 0.4$ and $dt = 0.001$. (a) Lyapunov characteristic exponents of the wandering chimera solution and the partial sums of the Lyapunov exponents $\Gamma_i = \sum_{k=1}^{i} \lambda_k$. (b) Power spectrum of displacements time series.

tion (3) are compared in Fig. 5(b). The probability distribution of displacements of chimera-like states resembles to the probability distribution of displacements of a Brownian motion. The rhythms of the displacements of a Brownian particle are completely determined by a random process (Wiener process [52]). However, unlike a Brownian motion, the self-correlation function $R(T) = \langle \Delta x(t) \Delta x(t+T) \rangle$ does not decrease despite the increasing of T, highlighting the memory effects of this motion. Moreover, the self-correlation shows an oscillatory behavior between a considerable maxima and minima values [see Fig. 5(c)]. Observe that $R(T)$ was measured using the Pearson correlation coefficient. Besides, we have plotted the distribution of displacement in the log-log scale, see insets in Fig. 5(b). This chart reveals that the displacement distribution corresponds to a truncated Gaussian distribution. This type of distribution is a consequence of the central limit theorem for a finite number of elements [54–56]. To check out this result, we have conducted different numerical simulations with very long periods and of different sizes and the distribution obtained is the same.

To characterize the statistical evolution of the displacement Δx in a given waiting time τ, we have monitored the evolution of the displacement distribution, the standard deviation σ, and the excess kurtosis κ. Fig. 6 summarizes this statistical analysis. Note that σ and κ show a linear and parabolic waiting time dependence, respectively. Similar dynamical behavior of σ was reported in phase coupled oscillators [46]. This type of dynamical statistical behavior is not peculiar of Brownian motion.

In brief, the position of the chimera-like state shows a wandering motion with a truncated Gaussian distribution of its displacement and memory effects.

To shed light on the dynamic nature of the wandering walk of chimera-like states, we will use tools from the theory of dynamic systems such as the power spectrum and Lyapunov exponents. These type of tools allows us to characterize the dynamics of modes and establish if the dynamics are of chaotic nature. When the largest Lyapunov exponent $\lambda_{\max}$ is negative, the system has a stationary equilibrium, for instance, homogeneous or pattern states. On the contrary, when it is positive, the system under study exhibits chaotic dynamics. Indeed, the Lyapunov spectrum characterizes the exponential sensibility to the initial conditions [57]. The analytical study of the Lyapunov spectrum is a titanic endeavor and in practice inaccessible. The numerical derivation of the exponents is a standard strategy. Indeed, it is necessary to spatially discretize the model Eq. (1). Hence, model (1) is approximated to a set of coupled ordinary differential equations, *discretized system*. From these equations, one can determine the discretized Jacobian at the chaotic solution, which characterizes the linear evolution of the state under study. To determine the Lyapunov exponents, we follow the linear evolution of an orthonormal deviation vectors basis of the discretized system. At every temporal evolution step, the deviation vectors are replaced by a new set of orthonormal vectors. From these orthonormalization procedures, Lyapunov exponents are estimated (see Ref. [58] for more details). We have calculated numerically the leading Lyapunov exponents of the chimera solution. Fig. 7 shows the positive Lyapunov spectrum of the chimera solution. From this spectrum, it is inferred that the strange attractor has at least 4 unstable directions. Note that few exponents are positive, which highlight a low-dimensional chaotic dynamics. In addition, one can determine the dimension of the strange attractor that characterizes the dynamics of the position of the chimera-like solution, using the Yorke-Kaplan conjecture [59]. The Yorke-Kaplan dimension is defined as $D_{YK} = n + \sum_{i=1}^{n} \lambda_i / |\lambda_{n+1}|$, where n is the largest integer such that $\lambda_1 + + \lambda_n > 0$. Fig. 7(a) shows the partial sum of the Lyapunov exponents $\Gamma_i = \sum_{k=1}^{i} \lambda_k$. From this chart, we found that $n = 10$. Then, the dimension is $D_{YK} \approx 10.005$. Besides, Fig. 7(b) displays the power spectrum of the temporal evolution of the displacements. The complex evolution of the wandering chimera state is revealed in a large number of frequency that is involved in the dynamics, which is typical of chaotic behaviors.

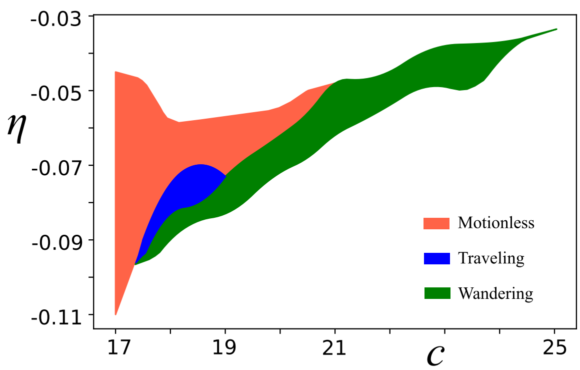

Fig. 8. (color online) Phase diagram of chimera states in parameter-space $\eta - c$ and for $\mu = -0.09$, $\nu = 1$, $b = -2$, $dx = 0.6$ and $dt = 0.01$. The green, blue and light red area account for the region where wandering, traveling, and motionless chimeras states are observed. The motionless and traveling chimera states are characterized by bounded and traveling centroid. (For interpretation of the references to color in this figure legend, the reader is referred to the web version of this article.)

Therefore, from the previous analysis, we infer that the wandering walk of the chimera-like solution is of a chaotic nature.

The wandering chimera-like states are observed in a wide range of parameters, which is a manifestation of the robust nature of these localized states. Fig. 8 shows the phase diagram of chimeras with wandering walks in $\eta - c$ parameters space. Hence, chimeras with wandering walks are observed in a wide region of the parameter space. It is important to note that these chimeras with wandering walks can coexist with motionless localized structures and confined chimeras.

In conclusion, we have shown that wandering dynamics of the position of chimera solutions in continuous spatially extended systems. These intriguing states are observed in the nonvariational Swift-Hohenberg equation, which is a prototype model of pattern formation. We have investigated the statistical and dynamical properties of wandering chimera states. The wandering walk of these solutions shows a truncated Gaussian distribution in its displacements. This property and the sensitivity to the initial conditions resemble a sort of Brownian motion. However, the wandering walk of the chimera states exhibits memory effects that are characterized by the self-correlation function. Besides, we have shown that the evolution of the position of wandering chimera-like state corresponds to chaotic behavior. To support this statement, the leading Lyapunov exponents were calculated.

Due to the generic character of the nonvariational Swift-Hohenberg equation, we expect the observation of wandering chimera-like states in a wide range of systems. In addition, we can take advantage of these wandering chimera-like states as Brownian motors [60] to induce propagation or control of coexisting localized structures. Finally, this work provides insights into novel ways of light beam generation with coexisting coherent and incoherent domains. The incoherent domain remains in a wandering motion. We expect that such kind of light beam will have significant and far-reaching ramifications in the development of novel and practical technological applications. Work in this direction is in progress.

Declaration of Competing Interest

The authors declare that they have no known competing financial interests or personal relationships that could have appeared to influence the work reported in this paper.

Acknowledgments

This work was supported by CONICYT under grant CONICYT-USA PII20150011. MGC and MAF also thank the Millennium Institute for Research in Optics (MIRO) FONDECYT Project no. 1180903 for financial support. AJA-S thanks financial support from Becas Conicyt 2015, Contract No 21151618.

References

[1] Prigogine I. Self-Organization in Non Equilibrium SystemsSelf-Organization in non equilibrium systems. New York: J. Wiley & Sons; 1977.
[2] Cross MC, Hohenberg PC. Pattern formation outside of equilibrium. Rev Mod Phys 1993;65:851.
[3] Pismen LM. Patterns and Interfaces in Dissipative DynamicsPatterns and interfaces in dissipative dynamics. Berlin, Heidelberg: Springer Series in Synergetics Springer; 2006.
[4] Descalzi O, Clerc M, Residori S, Assanto G. Localized States in Physics: Solitons and Patterns. New York: Springer; 2010.
[5] Purwins HG, Bödeker HU, Amiranashvili S. Dissipative solitons. Adv Phys 2010;59:485.
[6] edited by solitons Dissipative. From Optics to Biology and Medicine. Lecture Notes in Physics, 751 Springer, Heidelberg; 2008. edited by.
[7] Coullet P. Localized patterns and fronts in non equilibrium systems. Int J Bifurcation Chaos Appl Sci Eng 2002;12:2445.
[8] Turaev D, Radziunas M, Vladimirov AG. Chaotic soliton walk in periodically modulated media. Phys Rev E 2008;77:065201 R.
[9] Zambrini R, Papoff F. Signal Amplification and Control in Optical Cavities with Off-Axis Feedback. Phys Rev Lett 2007;99:063907.
[10] Staliunas K, Sanchez-Morcillo VJ. Spatial-localized structures in degenerate optical parametric oscillators. Phys Rev A 1998;57:1454.
[11] Haudin F, Rojas RG, Bortolozzo U, Clerc MG, Residori S. Vortex Emission Accompanies the Advection of Optical Localized Structures. Phys Rev Lett 2011;106:063901.
[12] Paulau PV, Gomila D, Ackemann T, Loiko NA, Firth WJ. Self-localized structures in vertical-cavity surface-emitting lasers with external feedback. Phys Rev E 2008;78:016212.
[13] Scroggie AJ, Firth WJ, Oppo GL. Cavity-soliton laser with frequency-selective feedback. Phys Rev A 2009;80:013829.
[14] Tlidi M, Vladimirov AG, Pieroux D, Turaev D. Spontaneous Motion of Cavity Solitons Induced by a Delayed Feedback. Phys Rev Lett 2009;103:103904.
[15] Alvarez-Socorro AJ, Clerc MG, Tlidi M. Spontaneous motion of localized structures induced by parity symmetry breaking transition. Chaos 2018;28:053119.
[16] Clerc MG, Petrossian A, Residori S. Bouncing localized structures in a liquid-crystal light-valve experiment. Phys Rev E 2005;71:015205 R.
[17] Durniak C, Taki M, Tlidi M, Ramazza PL, Bortolozzo U, Kozyreff G. Modulated optical structures over a modulationally stable medium. Phys Rev E 2005;72:026607.
[18] Kozyreff G, Chapman SJ, Tlidi M. Interaction of two modulational instabilities in a semiconductor resonator. Phys Rev E 2003;68:015201 R.
[19] Kozyreff G, Tlidi M. Nonvariational real Swift-Hohenberg equation for biological, chemical, and optical systems. Chaos 2007;17:037103.
[20] Verschueren N, Bortolozzo U, Clerc MG, Residori S. Spatiotemporal Chaotic Localized State in Liquid Crystal Light Valve Experiments with Optical Feedback. Phys Rev Lett 2013;110:104101.
[21] Nicolaou ZG, Riecke H, Motter AE. Chimera States in Continuous Media: Existence and Distinctness. Phys Rev Lett 2017;119:244101.
[22] Zhong L, Li Y, Chen Y, Hong W, Hu W, Guo Q. Chaoticons described by nonlocal nonlinear Schrödinger equation. Sci Rep 2017;7:41438.
[23] Verschueren N, Bortolozzo U, Clerc MG, Chaoticon Residori S. localized pattern with permanent dynamics. Phil Trans R Soc A 2014;372:20140011.
[24] Abrams DM, Strogatz SH. Chimera States for Coupled Oscillators. Phys Rev Lett 2004;93(17):174102.
[25] Kuramoto Y, Battogtokh D. Coexistence of Coherence and Incoherence in Nonlocally Coupled Phase Oscillators. Nonlinear Phenom Complex Syst (Minsk, Belarus) 2002;5:380.
[26] Clerc MG, Coulibaly S, Ferré MA, García-Ñustes MA, Rojas RG. Chimera-type states induced by local coupling. Phys Rev E 2016;93:052204.
[27] Clerc MG, Ferré MA, Coulibaly S, Rojas RG, Tlidi M. Chimera-like states in an array of coupled-waveguide resonators. Opt Lett 2017;42:2906–9.
[28] Clerc MG, Ferré MA, Coulibaly S, Rojas RG. Chimera states in a Duffing oscillators chain coupled to nearest neighbors. Chaos 2018;28:083126.
[29] Nicolaou ZG, Eroglu D, Motter AE. Multifaceted Dynamics of Janus Oscillator Networks. Phys Rev X 2019;9:011017.
[30] Bastidas VM, Omelchenko I, Zakharova A, Scholl E, Brandes T. Quantum signatures of chimera states. Phys Rev E 2015;92:062924.
[31] Lazarides N, Neofotistos G, Tsironis GP. Chimeras in SQUID metamaterials. Phys Rev B 2015;91:054303.
[32] Santos MS, Szezech JD, Borges FS, Iarosz KC, Caldas IL, Batista AM, et al. Chimera-like states in a neuronal network model of the cat brain. Chaos Solitons Fractals 2017:101.
[33] Larger L, Penkovsky B, Maistrenko Y. Virtual Chimera States for Delayed-Feedback Systems. Phys Rev Lett 2013;111:054103.
[34] Bera BK, Ghosh D. Chimera states in purely local delay-coupled oscillators. Phys Rev E 2016;93:052223.
[35] Gonzalez-Avella JC, Cosenza MG, Miguel MS. Localized coherence in two interacting populations of social agents. Phys A 2014;399:24.
[36] Sethia GC, Sen A. Chimera States: The Existence Criteria Revisited. Phys Rev Lett 2014;112:144101.

[37] Yeldesbay A, Pikovsky A, Rosenblum M. Chimeralike States in an Ensemble of Globally Coupled Oscillators. Phys Rev Lett 2014;112:144103.
[38] Hens CR, Mishra A, Roy PK, Sen A, Dana SK. Chimera states in a population of identical oscillators under planar cross-coupling. Pramana 2015;84:229–35.
[39] Laing CR. Chimeras in networks with purely local coupling. Phys Rev E 2015;92:050904 R.
[40] Hizanidis J, Lazarides N, Tsironis GP. Robust chimera states in SQUID metamaterials with local interactions. Phys Rev E 2016;94:032219.
[41] Sethia GC, Sen A, Johnston GL. Amplitude-mediated chimera states. Phys Rev E 2013;88:042917.
[42] Xie J, Knobloch E, Kao HC. Multicluster and traveling chimera states in nonlocal phase-coupled oscillators. Phys Rev E 2014;90:022919.
[43] Bera BK, Ghosh D, Banerjee T. Imperfect traveling chimera states induced by local synaptic gradient coupling. Phys Rev E 2016;94:012215.
[44] Hizanidis J, Panagakou E, Omelchenko I, Schöll E, Hövel P, Provata A. Chimera states in population dynamics: Networks with fragmented and hierarchical connectivities. Phys Rev E 2015;92:012915.
[45] Omel'chenko OEJ. Traveling chimera states. Phys A: Math Theor. J. Phys A 2019;52.
[46] Omel'chenko OE, Wolfrum M, Maistrenko YL. Chimera states as chaotic spatiotemporal patterns. Phys Rev E 2010;81:065201 R.
[47] Residori S, Petrossian A, Nagaya T, Clerc MG. Localized Structures and their Dynamics in a Liquid-Crystal-Light-Valve with Optical Feedback. JJ. Opt. B: Quantum Semiclass. Opt. 2004;6:S169.
[48] Burke J, Dawes JH. Localized states in an extended Swift–Hohenberg equation. SIAM J Appl Dyn Syst 2012;11:261.
[49] Swift J, Hohenberg PC. Hydrodynamic fluctuations at the convective instability. Phys Rev A 1977;15:319.
[50] Alvarez-Socorro AJ, Clerc MG, González-Cortés G, Wilson M. Nonvariational mechanism of front propagation: Theory and experiments. Phys Rev E 2017;95:010202 R.
[51] Houghton SM, Knobloch E. Swift-Hohenberg equation with broken cubic-quintic nonlinearity. Phys Rev E 2011;84:016204.
[52] Rudnick J, Gaspari G. Elements of the random walk. New York: Cambridge University Press; 2004.
[53] Fraser AM, Swinney HL. Independent coordinates for strange attractors from mutual information. Phys Rev A 1986;33:1134–40.
[54] Kaneko K. Globally coupled chaos violates the law of large numbers but not the central-limit theorem. Phys Rev Lett 1990;65:1391.
[55] Pikovsky AS, Kurths J. Do globally coupled maps really violate the law of large numbers? Phys Rev Lett 1994;72:1644.
[56] González JA, Moreno AJ, Guerrero LE. Non-invertible transformations and spatiotemporal randomness. Int J Bifurc Chaos Appl Sci Eng 2007:16.
[57] Pikovsky A, Politi A. Lyapunov exponents: a tool to explore complex dynamics. Cambridge University; 2016.
[58] Skokos CH. Dynamics of small solar system bodies and exoplanets. Springer; 2010. p. 63–135.
[59] Ott E. Chaos in dynamical systems. 2nd ed. Cambridge University; 2002.
[60] CVd Broeck, Kawai R, Meurs P. Microscopic analysis of a thermal Brownian motor. Phys Rev Lett 2004;93:090601.